JOURNAL OF MATERIALS SCIENCE 23 (1988) 1637–1642

Electron-beam melting and centrifugal splat-quenching technique for rapid solidification of titanium alloys

R. SESHADRI, R. V. KRISHNA RAO, R. V. KRISHNAN
Materials Science Division, National Aeronautical Laboratory, Bangalore 560 017, India
R. M. MALLYA
Department of Metallurgy, Indian Institute of Science, Bangalore 560 012, India

An electron-beam melting and centrifugal splat-quenching technique for the production of microflakes of Ti–6Al–4V (wt%) alloy quenched at an average cooling rate of about 10^5 K sec^{-1} is described. The effect of substrate angle on the shape, size, microstructure and average cooling rate of the flakes of major sieve fractions is discussed. Morphologies of particles of minor sieve fractions are dealt with briefly.

1. Introduction

The pioneering work of Duwez and his co-workers [1] on rapid quenching from the melt by splat cooling has led to the development of several related methods. All these methods have in common the feature of rapidly forming a thin layer of molten metal in good contact with a highly conducting solid metal heat sink. The centrifugal splat-quenching technique, based on a similar principle, has earlier been demonstrated to be capable of producing splat-cooled dense deposits [2] and flakes in bulk [3]. This technique has been evaluated for the production of rapidly solidified iron and aluminium alloys. However, it has not been widely used for titanium alloys although its use has been demonstrated for bulk splat cooling of reactive metals such as beryllium [4]. This is partly due to the reaction of molten titanium with crucible materials and with the environment, and partly due to the preference for spherical particulates for efficient consolidation by powder metallurgy techniques. Although many vacuum centrifugal atomization techniques [5–7] for near net-shape titanium metallurgy have emerged in the 1970s, the methods neither intend to nor produce a high quench rate.

In this paper we report the electron-beam melting and centrifugal splat-quenching technique for rapid solidification of titanium alloys and the influence of the substrate or heat sink angle (base angle of the frustum of a cone) on the shape, size, microstructure and cooling rate of the resulting rapidly solidified flakes of Ti–6Al–4V (wt%) conventional alloy. This alloy was selected for our studies because sufficient data on the effect of cooling rate on microstructure are available in the literature for comparison to evaluate the process.

The technique involves the melting of the tip of a pre-alloyed titanium rod by an electron beam and simultaneously rotating it about a vertical axis in vacuum. The resulting centrifugal spray of molten metal droplets flatten on impact with the surrounding stationary substrate and are quenched solid.

2. Equipment

The general arrangement of the experimental apparatus is shown in Fig. 1. This consists of a cylindrical vacuum chamber evacuated to about 10^{-2} Pa. The alloy to be atomized, in the form of a rod, is held vertically in a collet chuck mounted on a shaft. This shaft extends out of the bottom of the chamber through a differentially pumped rotary vacuum seal and is rotated by an external induction motor via belt and pulleys. A 15 kVA electron-beam gun mounted on top of the chamber is used for melting the tip of the rod. The copper sheet substrate (3 mm thick) in the form of a segment of the frustum of a cone, with a mechanically polished (centre line average of about 0.08 μm) inside impact surface, is positioned surrounding the rod. The impact position on the substrate is maintained at about 200 mm from the axis of the

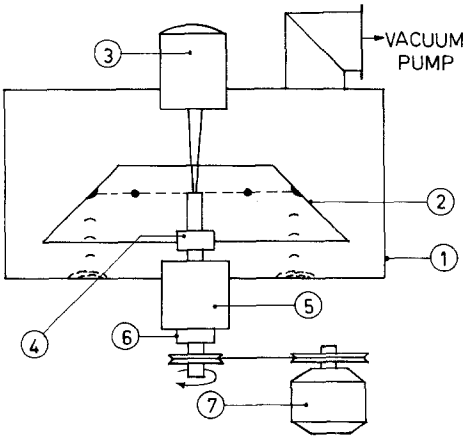

Figure 1 Schematic diagram of the electron-beam melting and centrifugal splat-quenching equipment. 1, vacuum chamber; 2, copper substrate; 3, electron-beam gun; 4, collet chuck; 5, bearing housing; 6, rotary vacuum seal; 7, electric motor.

0022–2461/88 $03.00 + .12

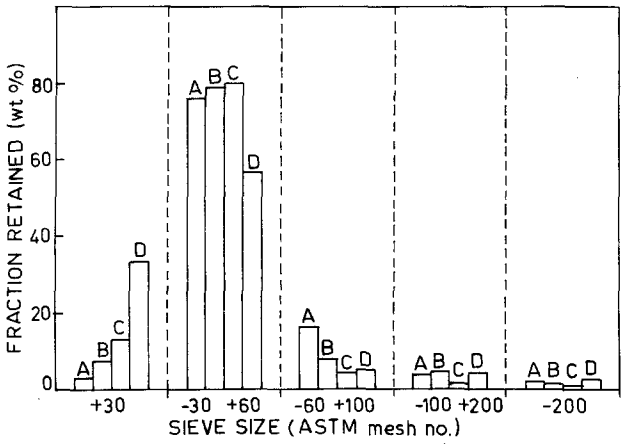

Figure 2 Sieve fractions obtained for different substrate angles: (A) 15°, (B) 30°, (C) 45°, (D) 60°.

rod at the time of starting the experiment for all the angled substrates.

3. Experimental procedure

The experiments were carried out with different angled substrates under identical operating conditions (rotational speed = 9400 r.p.m., rod diameter = 30 mm, melting rate = 2 kg h^{-1} and chamber vacuum = 1.3 × 10^{-2} Pa). These runs were conducted for short durations of approximately 45 sec to prevent over heating of the substrate. The microflakes collected below the impact position of the substrate were gathered and separated into five sieve fractions, as shown in Fig. 2, in a standard mechanical sieve shaker. The major sieve fractions were identified on the basis of the weight per cent of powder retained on the sieves. Scanning electron microscopy was employed to determine the surface microstructures, sizes and shapes of microflakes of the major sieve fractions and the morphologies of the particles of minor sieve fractions. Samples for surface microstructure studies were prepared by directly etching (with HF + HNO_3) the as-produced flakes. Cross-sectional microstructures were studied by optical microscopy from specimens prepared by mounting, polishing and etching the as-produced flakes. Thickness measurements were made on mounted, polished and unetched samples using a graduated ocular in an optical microscope. The average thickness of each flake was determined by taking the average of thickness measurements at equal intervals along its length or width. X-ray diffractometry was employed to determine the phases present and their crystal structures. Beta grain-size measurements were made using the linear intercept method.

4. Results and discussions

From the operating conditions stated in the previous section it was found that the direct drop formation mechanism was likely to be in operation during these runs [8]. This results in a bimodal particle-size distribution with the main and satellite particles forming the dominant and secondary modes, respectively. The median diameters of the dominant and secondary modes were determined by empirical relations [9] and were found to be approximately 265 and 115 μm, respectively.

The spherical molten metal droplets of centrifugal spray produced during these runs have flattened on impact with the substrates to form microflakes. The majority of the flakes were found to be detached from the substrates as soon as they solidify and collect on the chamber floor below the impact positions. The extensive splatting of the atomized droplets showed that the droplets were in a fully molten condition prior to their impact with the substrate.

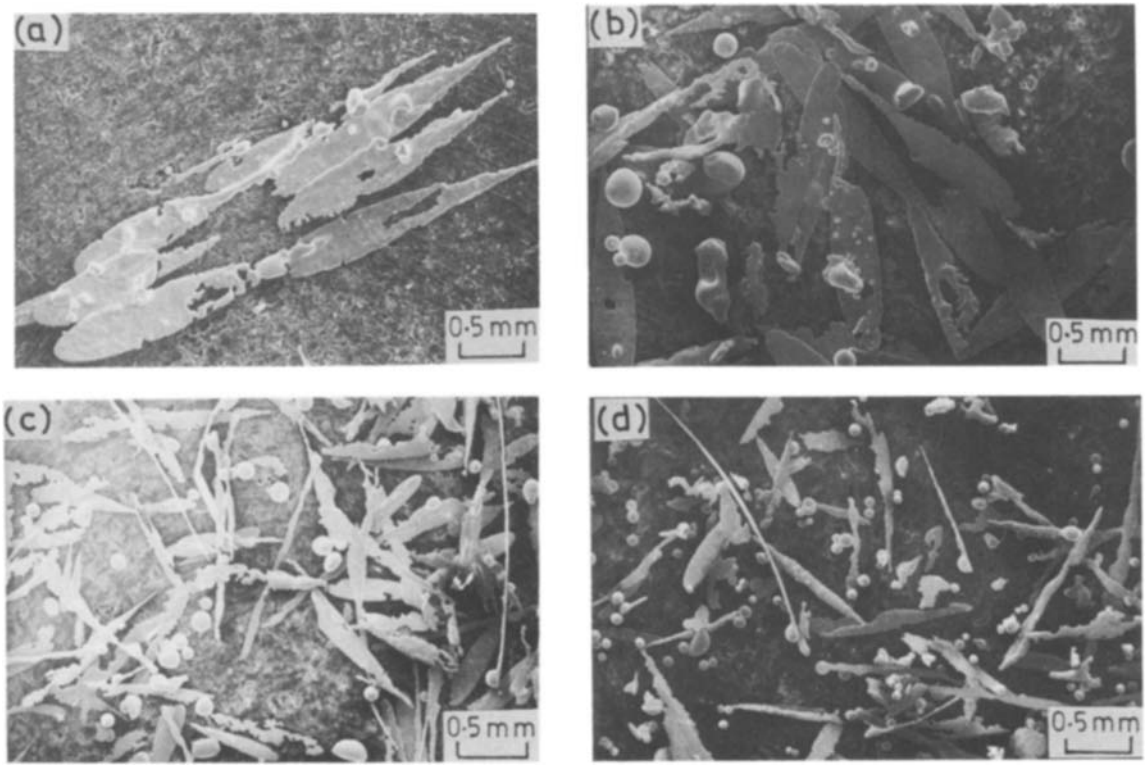

Figure 3 Morphologies of particles of minor fractions observed for 15° substrate angle: (a) + 30, (b) − 60 + 100, (c) − 100 + 200, (d) − 200.

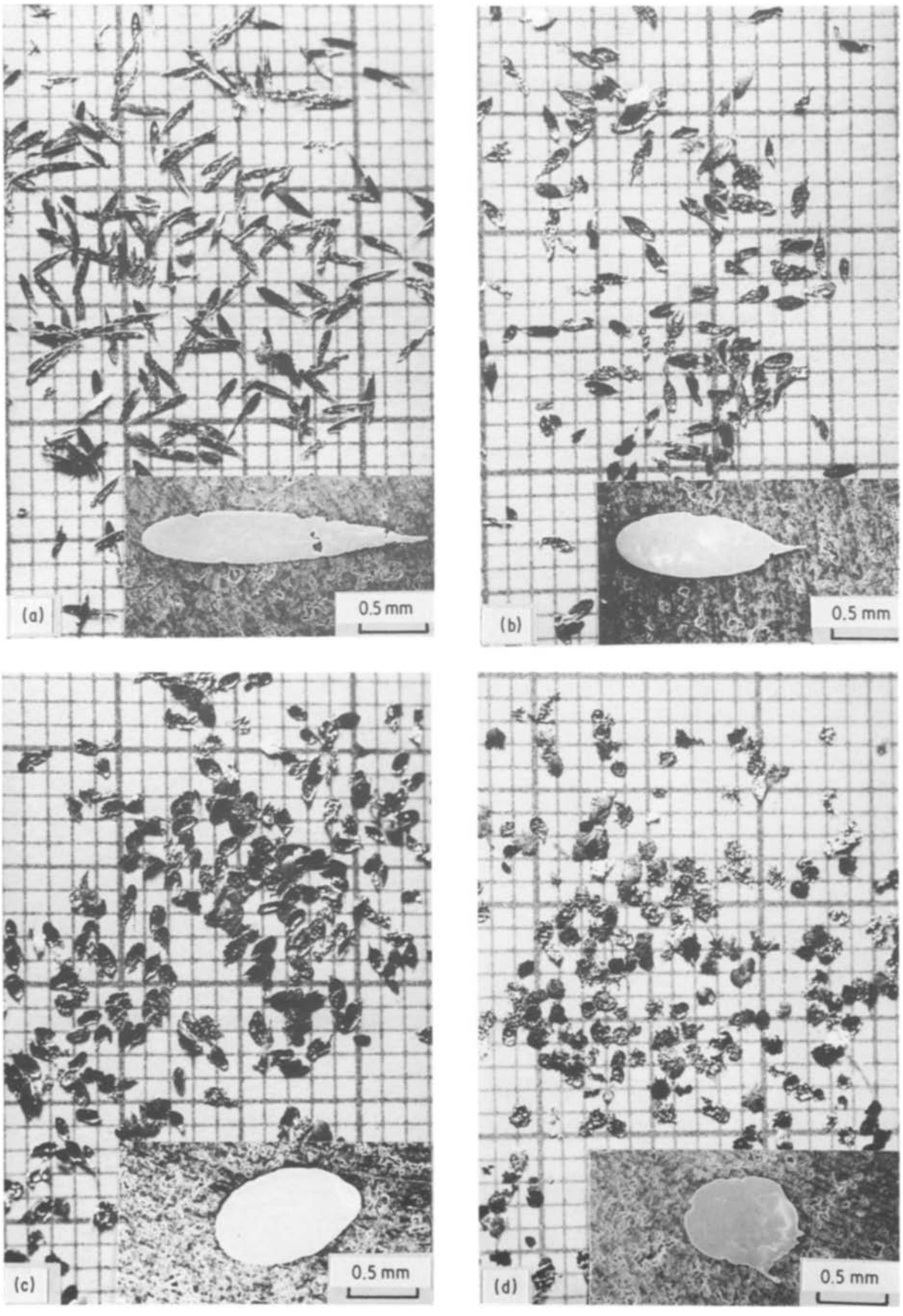

Figure 4 Shapes of microflakes (on millimetre graph sheet) of $-30 + 60$ fractions obtained for different substrate angles: (a) 15°, (b) 30°, (c) 45°, (d) 60° (inset shows individual particle at higher magnification).

4.1. Minor sieve fractions

A few flakes still adhering to the substrates were found to result in agglomerations due to the impact of subsequent droplets. Minor sieve fractions, $+30$, consisted of these agglomerates (Fig. 3a) and were found to increase in quantity with the increase in substrate angle.

Smaller satellite droplets, formed simultaneously with the main droplets, resulted in finer flakes after impact with the substrates. However, imperfect

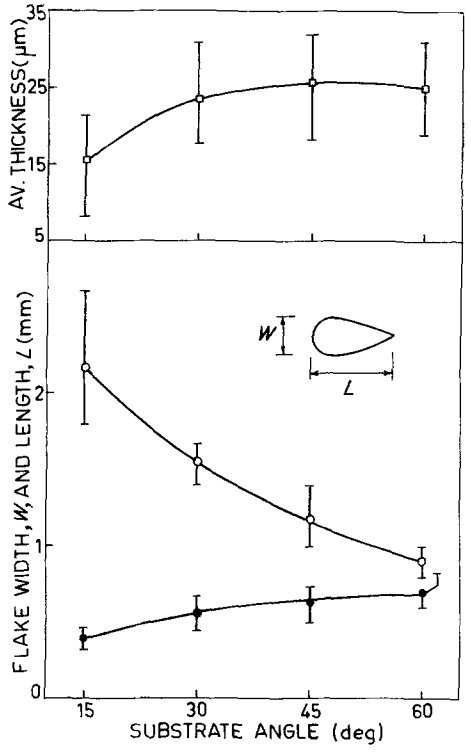

Figure 5 Variation of (●) width, (○) length and (□) average thickness of flakes of −30 + 60 fractions with the substrate angle.

substrate surface conditions at isolated places have probably resulted in a few irregular shaped finer flakes. Secondary atomization, occurring during spreading of the droplets on the substrates, resulted in spherical, hemispherical, filamentary and sperm-like particles. Minor sieve fractions (−60 + 100, −100 + 200, and −200) consisted of particles with these features (Figs 3b to d).

4.2. Major sieve fractions

The main droplets formed during centrifugal atomization, have resulted in microflakes having uniform shape and size. The major sieve fractions, −30 + 60, consisted of these microflakes. The shape was found to change gradually from elongated to nearly circular as the substrate angle was changed from 15° to 60° as shown in Fig. 4. Although the shapes of the flakes

TABLE I Substrate angle (θ) and corresponding measured average beta grain size (L) of flakes of −30 + 60 fractions

θ (deg)	L (μm)
15	31 ± 7
30	44 ± 5
45	35 ± 6
60	51 ± 12

shown in Figs 4a and d resemble somewhat the shapes reported elsewhere [10], the substrate conditions under which they were produced were not reported earlier. The length and width of these flakes were found to decrease and increase, respectively, with the increase in substrate angle as shown in Fig. 5. These variations may be due to the changes in the magnitudes of the components of impact velocity along and normal to the substrate with the change in substrate angle.

Macroscopic examination revealed perforations in approximately 30% to 40% of the flakes produced. These perforations may be due to the imperfect surface conditions and/or imperfect spreading of the molten metal droplets at isolated places on the impact surface of the substrates. The cross-section of these flakes along the length and width (Fig. 6) showed smooth surfaces on the substrate sides and surface irregularities on the free sides. An abrupt large increase in thickness was observed in some flakes in isolated places (up to twice the average thickness). Similar variations were observed by Williams and Jones [11] on splats of Sn–Pb and Al–Si alloys. The average thickness measured on cross-sections of the flakes (excluding these isolated places) was found to vary with substrate angle, as shown in Fig. 5.

The microstructures of all the as-produced flakes were martensitic and many martensitic plates were found to traverse the width of beta grains on the surface of the flakes, as shown in Fig. 7. The majority of beta grains were found to extend through the thickness of individual flakes with the principal growth direction perpendicular to the flake surface. This implies that heat extraction has occurred in the

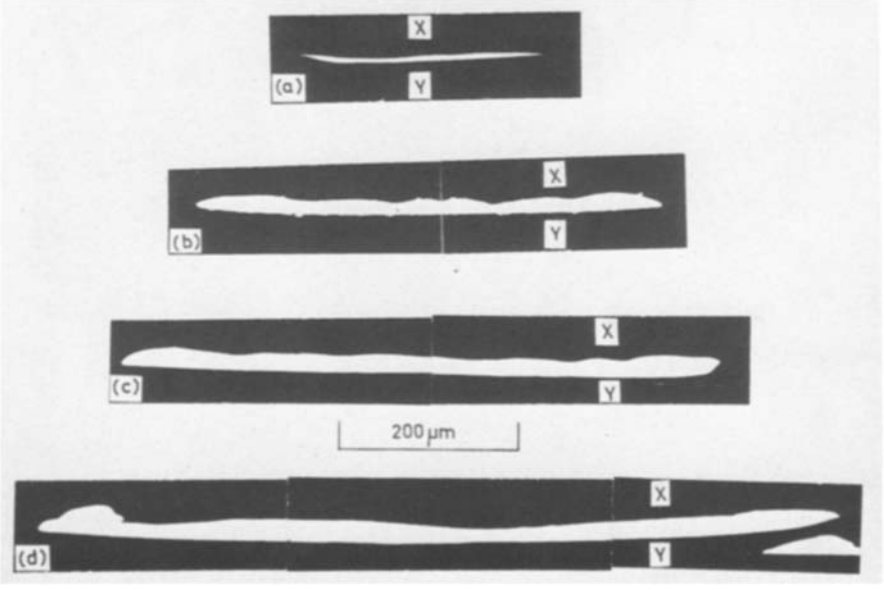

Figure 6 Cross-section of unetched flakes of −30 + 60 fraction (along width) for different substrate angles: (a) 15°, (b) 30°, (c) 45°, (d) 60° (X and Y are free and substrate sides, respectively).

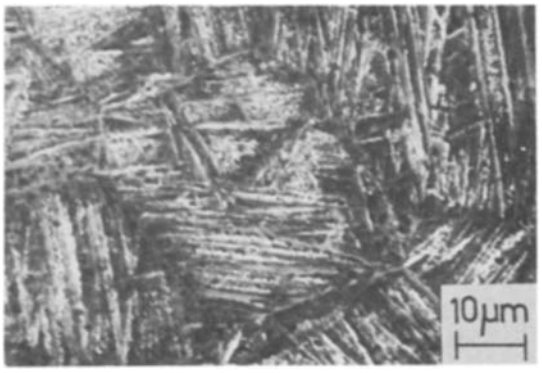

Figure 7 Typical surface microstructure of flakes of −30 + 60 fraction.

direction normal to the flake surface into the substrate. This is typical of rapidly solidified flakes or splats [12, 13] except that in the present case the average beta grain size was larger than the corresponding flake thickness. While in a few grains martensite plates extended across the diameter (Fig. 8a), in the majority of grains many martensite plates extended through the thickness of individual flakes (Fig. 8b). X-ray powder diffraction patterns, obtained from these flakes, showed the presence of single martensitic phase with h c p crystal structure.

The microflakes produced were all solidified by conduction heat transfer to the copper substrate. Hence cooling rates depend mainly on flake thickness, z, and heat transfer coefficient, h, and conditions of Newtonian or ideal cooling apply depending on Nusselt number N ($N = hz/k$ where k is the thermal conductivity) [14]. Assuming an average value of h of $0.1\,\mathrm{W\,mm^{-2}\,K^{-1}}$ [15] in the absence of a reliable measurement for titanium or a titanium alloy, N varies between 0.026 and 0.106 for the present values of average flake thickness (0.008 to 0.032 mm) and $k \sim 0.03\,\mathrm{W\,mm^{-1}\,K^{-1}}$ for titanium at its melting point [16]. As a reasonable approximation, applying Newtonian cooling conditions for these values of N, the cooling rate, $\dot{T}$, can be estimated by [17]

$$\dot{T} = \frac{h(T - T_A)}{\varrho c z}$$

where T is the particulate temperature, T_A is the ambient temperature, and c, ϱ are the specific heat and density of the particulate, respectively. Substituting in this equation $c = 0.1672\,\mathrm{cal\,g^{-1}\,K^{-1}}$ and $\varrho = 4.35\,\mathrm{g\,cm^{-3}}$ for titanium at its melting point ($T = 1953\,\mathrm{K}$) [16] together with $T_A = 293\,\mathrm{K}$, gives $\dot{T}$ between 1.7×10^6 and $6.8 \times 10^6\,\mathrm{K\,sec^{-1}}$ for the observed total range of average thickness. It is also evident from this equation and Fig. 5 that smaller substrate angles yield flakes cooled at higher rates.

Beta grain sizes, L, measured for different substrate angles, θ, are shown in Table I. Although only marginal differences were observed it is seen that L decreases with decreasing θ and hence with decreasing z and increasing $\dot{T}$. The cooling rates determined from these measured values of L and previously established beta grain size/cooling rate correlation ($L = 3.1 \times 10^6\,\dot{T}^{-0.93}$) [18] fall in the range 1.4×10^5 and $2.4 \times 10^5\,\mathrm{K\,sec^{-1}}$. These are less than the calculated cooling rates by at least a factor of ten. This discrepancy could be due to the following reasons.

(a) The value of h assumed in calculating cooling rates may be higher than that applicable in the present case due to the probable poor thermal contact between the flake and the substrate and also the possible presence of a layer of adsorbed air and an oxide film on the substrate.

(b) The thermal and gravity effects might have led to the premature detachment of flakes from the substrates while still at elevated temperature, giving an insufficient residence time for the flakes to cool to room temperature by conductive heat transfer to the substrate alone.

In view of the uncertainties in calculating the exact cooling rates, and the fact that variable thermal contact ensures that thinner specimens are not invariably the most rapidly quenched ones [19–21], an average cooling rate of about $10^5\,\mathrm{K\,sec^{-1}}$ appears to be a reasonable estimate in the present case.

5. Conclusions

From the above experimental work it is concluded that:

1. microflakes of Ti–6Al–4V (wt %) alloy quenched at an average cooling rate of about $10^5\,\mathrm{K\,sec^{-1}}$ can be produced by this technique;

2. the shape, length, width, thickness, beta grain size and cooling rate of the flakes produced depend on the substrate angle. As the substrate angle increases the shape changes from elongated to nearly circular

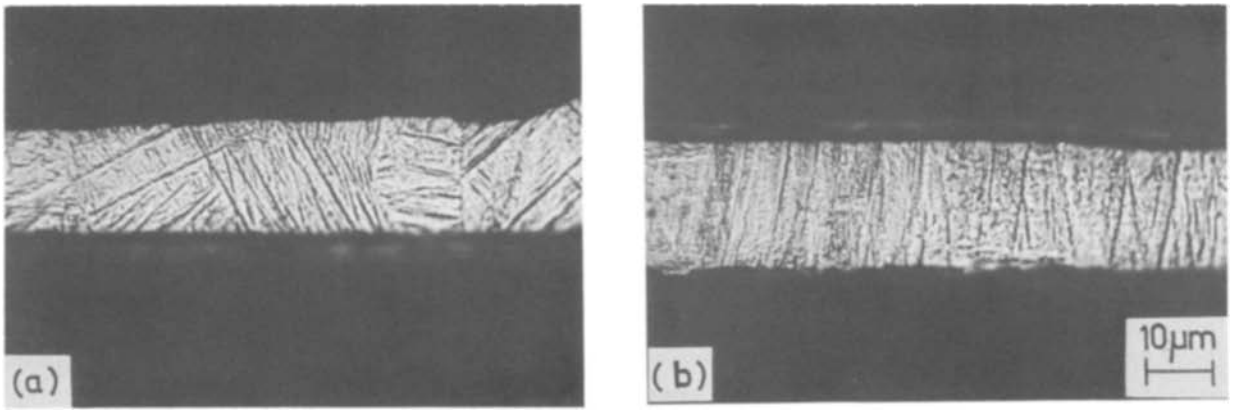

Figure 8 Typical cross-sectional microstructure of flakes of −30 + 60 fraction (top and bottom surfaces are free and substrate sides, respectively).

and the length and width of the flakes decreases and increases, respectively. Lower substrate angles yield flakes having smaller thickness, smaller beta grain size and higher cooling rate;

3. with the high atomization rate possible, the process appears suitable for bulk production of rapidly solidified microflakes of titanium and other reactive metals and their alloys in vacuum.

Acknowledgements

The authors acknowledge helpful discussions with Dr A. C. Raghuram, Dr A. K. Singh and Prof. S. Ranganathan, and thank the Defence Metallurgical Research Laboratory for providing them with pre-alloyed titanium rods, Mr M. A. Venkataswamy and Mr T. A. Bhaskaran for SEM work and Dr C. Balasingh for X-ray analysis. The help of Mr M. Maikandan, Mr Srinivasa Reddy and Mr Maria Sylvester in experimental work is also gratefully acknowledged.

References

1. W. KLEMENT, R. H. WILLENS and P. DUWEZ, *Nature* **187** (1960) 869.
2. A. R. E. SINGER and S. E. KISAKUREK, *Metals Technol.* **12** (1976) 565.
3. H. JONES and M. H. BURDEN, *J. Phys. E Sci. Instrum.* **4** (1971) 671.
4. A. R. KAUFMANN and W. C. MULLER, USAEC Report NMI-1262 (1964).
5. J. DECOURS, J. DEVILLARD and G. STAINFORT, in AGARD Conference Proceedings No. 200, "Advanced Fabrication Techniques in Powder Metallurgy and their Economic Implications", Ottawa (1976) p. 1.
6. H. STEPHEN, H. SCHMITT and R. RUTHARDT, *ibid.* No. 256, "Advanced Fabrication Processes", Florence (1978) p. 17.
7. R. SUNDARESAN, R. SESHADRI, R. V. KRISHNAN, A. C. RAGHURAM, W. KRISHNASWAMY and N. C. BIRLA, in 10th Plansee Conference Proceedings, Vol. 2 (1981) p. 385.
8. B. CHAMPAGNE and R. ANGERS, *Powder Met. Int.* **16** (1984) 125.
9. *Idem*, in "Modern Development in Powder Metallurgy", Vol. 12, edited by Henry H. Hausner and Pierre W. Tanbenblat (MPIF and APMI, Princeton, New Jersey, 1981) p. 83.
10. H. STEPHEN and J. K. FISCHHOF, *ibid.* Vol. 9 (1977) p. 183.
11. C. A. WILLIAMS and H. JONES, *Mater. Sci. Engng* **19** (1975) 293.
12. H. JONES, "Rapid Solidification of Metals and Alloys", Monograph No. 8 (Institution of Metallurgists, London, 1982).
13. J. WOOD and I. SARE, *Met. Trans.* **6A** (1975) 2153.
14. R. C. RUHL, *Mater. Sci. Engng* **1** (1967) 313.
15. H. JONES, in "Rapidly Quenched Metals", edited by N. J. Grant and B. C. Giessen (MIT, Cambridge, Massachussetts, 1976) p. 1.
16. Y. S. TOULOUKIAN and C. Y. HO, "Thermophysical Properties of Matter", (IFI Plenum, New York, 1972).
17. R. SCHUHMANN Jr, "Metallurgical Engineering", Vol. 1 (Addison-Wesley, Reading, Massachusetts, 1952) p. 260.
18. T. F. BRODERICK, F. H. FROES, A. G. JACKSON and H. JONES, *Met. Trans.* **16A** (1985) 1951.
19. M. LEBO and N. J. GRANT, *ibid.* **5** (1974) 1547.
20. A. TONEJC, *ibid.* **2** (1971) 437.
21. K. KRANJE and M. STUBIČAR, *ibid.* **4** (1973) 2631.

Received 23 April
and accepted 22 September 1987